Raman Optical Activity in the Skeletal Motions of (+)-(3R)-Methylcyclohexanone. Chiral Mixing of Inherently Achiral Vibrations

Teresa B. Freedman,* James Kallmerten, Carl G. Zimba, William M. Zuk, and Laurence A. Nafie*

Contribution from the Department of Chemistry, Syracuse University, Syracuse, New York 13210. *Received August 26, 1983*

Abstract: The Raman and Raman optical activity (ROA) spectra of (+)-(3*R*)-methylcyclohexanone in the 100–650-cm^{-1} region are assigned to 11 skeletal motions based on Raman studies and normal coordinate analysis of the parent compound and five specifically deuterated isotopomers. The origin of the three prominent bisignate ROA couplets observed in this region is explained in terms of chiral vibrational perturbation due to the presence of the methyl group which mixes the inherently achiral A′ and A″ skeletal modes of cyclohexanone. Molecular orbital intensity calculations using the Raman atomic polar tensor model for ROA show good agreement with experiment for the skeletal vibrations.

Introduction

Raman optical activity (ROA),[1-3] the difference in Raman scattering by chiral molecules of left vs. right circularly polarized excitation, provides both stereochemical information on chiral molecules in solution and information concerning vibrational assignments in complex molecules of low symmetry. Numerous correlations between ROA features and absolute configurations have been made.[1-10] These do not, however, rely on vibrational assignments, and the nature of the vibrational motion giving rise to most ROA features remains unknown.

The sources of Raman optical activity have been discussed from two points of view. Descriptively, one can consider the generation of ROA by the coupling of vibrations on identical, chirally disposed achiral groups, and by the splitting of degenerate modes or the coupling of achiral nondegenerate vibrations by chiral peturbations.[2,3] Computational models from which the sign and magnitude of ROA features can be calculated, requiring accurate knowledge of nuclear trajectories, have also been proposed. These models include the two-group model,[2,11] the atom–dipole interaction model,[12] the bond polarizability theory,[3,13] the localized molecular orbital[14] and equivalent orbital polarizability models,[15] and the Raman atomic polar tensor model.[16] Success in applying these models has been limited. The main difficulty in the interpretation of ROA spectra from either a descriptive or computational approach has been the speculative nature of proposed vibrational assignments and the imprecise force fields used to generate the calculated normal modes. Vibrational optical activity calculations are known to place more stringent requirements on the force field than general frequency agreement or descriptive assignments require.

We recently proposed the atomic polar tensor (APT)[16] models for vibrational circular dichroism (VCD) and Raman optical activity as an efficient molecular orbital method for calculating infrared, Raman, VCD, and ROA intensities for all the normal modes of a molecule in one concerted calculation. We have previously tested and evaluated[16] the APT method for VCD using CNDO wave functions and have found good agreement with experiment in the CH stretching region, especially for vibrations involving nuclear motion distributed among several internal coordinates. One objective of our current research has been to test the APT method for ROA as well.

The ROA spectrum[2] of (+)-(3*R*)-methylcyclohexanone lends itself well to such a study. The 100–650-cm^{-1} region in particular consists of distinct ROA features, including couplets, which correspond to nearly every observed Raman band in the region. Sources of the ROA couplets in this spectrum have been previously explored using the descriptive mechanisms discussed above,[2] and attempts have been made to apply both the atom–dipole interaction model[17] and the bond polarizability theory[18] to 3-methylcyclohexanone. These previous analyses, however, have relied on inaccurate or incomplete descriptions of the normal modes.

In the current study we have carefully refined the force field for the skeletal vibrations of 3-methylcyclohexanone using Raman frequencies for several specifically deuterated isotopomers. From the resulting calculated nuclear trajectories for the skeletal motions, we have been able both to give a complete descriptive interpretation of the sources of ROA intensity in these modes and to successfully calculate the intensities of ROA features using the APT model of ROA.

Experimental Section

3-Methylcyclohexanone (Aldrich, 99%) was distilled prior to use to remove fluorescent photodecomposition products. Five specifically deuterated isotopomers were synthesized in our laboratories. 3-methlcyclohexanone-2,2,6,6-d_4 was prepared by exchange at the reactive 2 and 6 positions following the procedure used by Fuhrer et al. for cyclohexanone-α-d_4.[19] Although in our case the organic and aqueous phases in the reaction mixture were immiscible, the deuteration was complete after refluxing. The preparation of the deuterated species 3-methylcyclohexanone-5,5-d_2, 3-methylcyclohexanone-4,4-d_2, 3-methylcyclohexanone 3-d_1, and 3-(*methyl*-d_3)-cyclohexanone has been communicated separately.[20] Isotopic purity of the deuterated products was greater than 95%, based on NMR and mass spectral analysis.

(1) Barron, L. D. *Acc. Chem. Res.* **1980**, *13*, 90. Barron, L. D. "Molecular Light Scattering and Optical Activity"; Cambridge University Press: Cambridge, England, 1982.
(2) Barron, L. D. In "Advances in Infrared and Raman Spectroscopy"; Clark, R. J. H., Hester, R. E., Eds.; Heyden: London, 1978; Vol. 4, p 271.
(3) Barron, L. D. In "Optical Activity and Chiral Discrimination"; Mason, S. F., Ed.; D. Reidel: Dordrecht, 1979; p 219.
(4) Hug, W.; Kint, S.; Bailey, G. F.; Scherer, J. R. *J. Am. Chem. Soc.* **1975**, *97*, 5589.
(5) Hug, W.; Surbeck, H. *Chem. Phys. Lett.* **1979**, *60*, 186.
(6) Brocki, T.; Moskovits, M.; Bosnich, B. *J. Am. Chem. Soc.* **1980**, *102*, 495.
(7) Boucher, H.; Brocki, T. R.; Moskovits, M.; Bosnich, B. *J. Am. Chem. Soc.* **1977**, *99*, 6870.
(8) Hug, W.; Kamatari, A.; Srinivasan, K.; Hansen, H. J.; Sliwka, H.-R. *Chem. Phys. Lett.* **1980**, *76*, 469.
(9) Polavarapu, P. L.; Diem, M.; Nafie, L. A. *J. Am. Chem. Soc.* **1980**, *102*, 5449.
(10) Barron, L. D.; Clark, B. P.; *J. Chem. Soc., Perkin Trans. 2* **1979**, 1170.
(11) Gohin, A.; Moskovits, M. *J. Am. Chem. Soc.* **1981**, *103*, 1660.
(12) Prasad, P. L.; Nafie, L. A. *J. Chem. Phys.* **1979**, *70*, 5582.
(13) Clark, B. P.; Barron, L. D. *Mol. Phys.* **1982**, *46*, 839.
(14) Nafie, L. A.; Freedman, T. B. *J. Chem. Phys.* **1981**, *75*, 4847.
(15) Polavarapu, P. L. *J. Chem. Phys.* **1982**, *77*, 2273.
(16) (a) Freedman, T. B.; Nafie, L. A. *J. Chem. Phys.* **1983**, *78*, 27; **1983**, *79*, 1104. (b) Freedman, T. B.; Nafie, L. A. *J. Phys. Chem.*, in press.
(17) Polavarapu, P. L.; Nafie, L. A. *J. Chem. Phys.* **1980**, *73*, 1567.
(18) Barron, L. D.; Clark, B. P. *J. Raman. Spectrosc.* **1982**, *13*, 155.
(19) Fuhrer, H.; Kartha, V. B.; Krueger, P. J.; Mantsch, H. H.; Jones, R. N. *Chem. Rev.* **1972**, *72*, 439.
(20) Kallmerten, J. *J. Labelled Compd. Radiopharm.* **1983**, *20*, 923.

0002-7863/84/1506-1244$01.50/0

The Raman spectra were obtained with a Spectra-Physics Model 164-3 argon ion laser, a Spex 1401 double monochromator, a cooled RCA 31034 GaAs photomultiplier tube, and a Pacific Model 110 photometer. The scattered light was collected perpendicular to the excitation at $f/1.3$ by a camera lens which also focused the light at the entrance slit of the monochromator. All spectra were acquired with 514.5-nm excitation at approximately 2 cm^{-1} spectral resoltuion using a scan speed of 2 cm/s and a time constant of approximately 10 s. The parent and 2,6-deuterated samples were freshly distilled and transferred to sealed vials in which the spectra were measured with 400-mW power at the sample. The remaining samples were purified by preparative gas chromatography using a 50-cm OV-101 column and oven temperature 65 °C. The effluent was trapped in liquid nitrogen cooled borosilicate U-tubes which were sealed prior to measuring the Raman spectra at an incident power of 100 mW. Typical sample volumes were 0.5 mL for the parent and 2,6-deuterated samples and 10 μL for the other samples.

The depolarized ROA spectrum of (+)-(3*R*)-methylcyclohexanone (100–1800 cm^{-1}) has been reported and discussed previously[2,3,21,22] by Barron. For the purposes of our analysis, we have redrawn the region between 100 and 600 cm^{-1} using a linear ordinate scale and defining ROA in terms of $I_L - I_R$ rather than $I_R - I_L$ as in Barron's reports. For exact details of the ROA spectrum we refer to the original published experimental spectra of Barron.

Calculations were carried out on a Dec 10 computer system using normal coordinate analysis programs in both internal and Cartesian coordinates and a CNDO/2 molecular orbital program[23] modified for gradient and electric field perturbation calculations and VOA intensity calculations as described previously.[16]

The stereoprojections of 3-methylcyclohexanone were drawn in our laboratory from the equilibrium and the calculated vibrationally displaced geometries by rotating the coordinate axes and scaling the relative displacements to give a clear view of the nuclear motions. The scale factor used for the methyl torsion mode was smaller by a factor of 3 than for the remaining modes.

Theoretical Background and Models

Intensity Expressions. Raman optical activity is measured as the difference in Raman scattering intensity for left vs. right circularly polarized excitation and is expressed by the chirality number[5]

$$q = (I_L - I_R)/\tfrac{1}{2}(I_L + I_R) \tag{1}$$

In terms of the transition matrix elements between levels i and f for the polarizability tensor components, $\alpha_{\alpha\beta}$, the magnetic dipole optical activity tensor components, $G'_{\alpha\beta}$, and the electric quadrupole optical activity tensor components $A_{\alpha\beta\gamma}$, the chirality number for depolarized ROA is[2,5]

$$q_P = \left(\frac{-4}{c}\right)\frac{3(\alpha_{\alpha\beta})_{if}(G'_{\alpha\beta})_{fi} - (\alpha_{\alpha\alpha})_{if}(G'_{\beta\beta})_{fi} - \tfrac{1}{3}\omega(\alpha_{\alpha\beta})_{if}\epsilon_{\alpha\gamma\delta}(A_{\gamma\delta\beta})_{fi}}{3(\alpha_{\lambda\mu})_{if}(\alpha_{\lambda\mu})_{fi} - (\alpha_{\lambda\lambda})_{if}(\alpha_{\mu\mu})_{fi}} \tag{2}$$

where ω is the incident frequency. In this expression and those to follow, we use Cartesian component notation, wherein Greek subscripts denote Cartesian directions, a repeated Greek subscript implies summation over the three Cartesian components, and $\epsilon_{\alpha\beta\gamma}$ is the unit alternating tensor, equal to 1 or −1 if $\alpha\beta\gamma$ is an even or odd permutation of the order xyz, respectively, and 0 if any two subscripts are the same.

According to the polarizability theory, from eq 1 we see that the ROA intensity for the fundamental of normal mode Q_a is determined by terms such as[2]

$$\langle a_0|\alpha_{\alpha\beta}|a_1\rangle\langle a_1|\alpha_{\alpha\beta}|a_0\rangle = \frac{\hbar}{2\omega_a}\left(\frac{\partial\alpha_{\alpha\beta}}{\partial Q_a}\right)_0^*\left(\frac{\partial\alpha_{\alpha\beta}}{\partial Q_a}\right)_0 \tag{3a}$$

$$\langle a_0|\alpha_{\alpha\beta}|a_1\rangle\langle a_1|G'_{\alpha\beta}|a_0\rangle = \frac{\hbar}{2\omega_a}\left(\frac{\partial\alpha_{\alpha\beta}}{\partial Q_a}\right)_0^*\left(\frac{\partial G'_{\alpha\beta}}{\partial Q_a}\right)_0 \tag{3b}$$

$$\langle a_0|\alpha_{\alpha\beta}|a_1\rangle\langle a_1|\epsilon_{\alpha\gamma\delta}A_{\gamma\delta\beta}|a_0\rangle = \frac{\hbar}{2\omega_a}\left(\frac{\partial\alpha_{\alpha\beta}}{\partial Q_a}\right)_0^*\epsilon_{\alpha\gamma\delta}\left(\frac{\partial A_{\gamma\delta\beta}}{\partial Q_a}\right)_0 \tag{3c}$$

Chiral Perturbation of Inherently Achiral Vibrations. The model we describe here to understand the generation of ROA in chiral molecules is to view the normal modes as chirally perturbed inherently achiral vibrations. This source of conservative ROA couplets was first considered by Barron[2] although there has not previously been unequivocal evidence that such coupling is in fact responsible for observed ROA features.

We first review the symmetry requirements for ROA,[2] that is, for nonzero products in eq 3a–c. The tensor element $\alpha_{\alpha\beta}$ transforms as the product of two dipole moment components $\mu_\alpha\mu_\beta$, and both $G'_{\alpha\beta}$ and $\epsilon_{\alpha\gamma\delta}A_{\gamma\delta\beta}$ transform as the product of an electric and a magnetic dipole moment component $\mu_\alpha m_\beta$. A normal mode Q_a will exhibit ROA if the same components $\alpha_{\alpha\beta}$ and $G'_{\alpha\beta}$ both belong to the irreducible representation of Q_a, which we denote as Γ_a. In the chiral point groups all Raman active vibrations exhibit ROA; in the nonchiral point groups, $\alpha_{\alpha\beta}$ and $G'_{\alpha\beta}$ always belong to different irreducible representations.

We now consider two inherently achiral nondegenerate vibrations Q_a and Q_b with ground vibrational states $|a_0\rangle$ and $|b_0\rangle$ where, for example, Q_a, α_{xz}, and G'_{yz} belong to Γ_a, and Q_b, α_{yz}, and G'_{xz} belong to a different representation Γ_b. A chiral vibrational perturbation V with

$$\langle a_1b_0|V|a_0b_1\rangle \neq 0 \tag{4}$$

will produce coupled modes with excited vibrational states

$$|1_+\rangle = c_1|a_1b_0\rangle + c_2|a_0b_1\rangle \tag{5a}$$

$$|1_-\rangle = c_2|a_1b_0\rangle - c_1|a_0b_1\rangle \tag{5b}$$

This coupling generates contributions to ROA intensity through products of the form

$$\langle 0|\alpha_{xz} + \alpha_{yz}|1_\pm\rangle\langle 1_\pm|G'_{xz} + G'_{yz}|0\rangle = \pm\frac{\langle a_1b_0|V|a_0b_1\rangle}{\hbar\omega_{a_1b_1}} \times (\langle a_0|\alpha_{xz}|a_1\rangle\langle b_1|G'_{xz}|b_0\rangle + \langle b_0|\alpha_{yz}|b_1\rangle\langle a_1|G'_{yz}|a_0\rangle) \tag{6}$$

which is observed as equal and opposite optical activity in the two bands. A similar couplet can arise through the mixing of more than two modes due to chiral terms in the vibrational Hamiltonian if the resultant vibrations consist of symmetric and antisymmetric combinations of motions of two appropriate symmetry species.

The Raman Atomic Polar Tensor Model. The analysis of the previous section, while quite useful for descriptive interpretation and assignments of ROA spectra (see below), provides no information as to the absolute sign and magnitude of the ROA features. Numerical calculation of ROA requires alternative methods, and we have previously proposed a molecular orbital model of ROA and VCD, the atomic polar tensor model.[16] In the ROA–APT model the normal coordinate derivatives of $G'_{\alpha\beta}$ and $A_{\alpha\beta\gamma}$ required in eq 3a–c are derived from the equilibrium nuclear positions $\mathbf{R}_{n,0}$, the nuclear trajectories $s_{n\alpha} = (\partial\mathbf{R}_n/\partial Q_a)_0$ and the equilibrium Cartesian displacement derivatives of $\alpha_{\alpha\beta}$,

$$\left(\frac{\partial G'_{\alpha\beta}}{\partial Q_a}\right)_0 = \omega_a\sum_n -\tfrac{1}{2}\epsilon_{\beta\gamma\delta}s_{na,\rho}R_{n0,\gamma}\left(\frac{\partial\alpha_{\delta\alpha}}{\partial R_{n\rho}}\right)_0 \tag{7a}$$

$$\left(\frac{\partial A_{\alpha\beta\gamma}}{\partial Q_a}\right)_0 = \sum_n s_{na,\rho}\left[\frac{3}{2}R_{n0,\beta}\left(\frac{\partial\alpha_{\gamma\alpha}}{\partial R_{n\rho}}\right)_0 + \frac{3}{2}R_{n0,\gamma}\left(\frac{\partial\alpha_{\beta\alpha}}{\partial R_{n\rho}}\right)_0 - R_{n0,\delta}\left(\frac{\partial\alpha_{\delta\alpha}}{\partial R_{n\rho}}\right)_0\delta_{\beta\gamma}\right] \tag{7b}$$

The Raman atomic polar tensor elements $(\partial\alpha_{\alpha\beta}/\partial R_{n\rho})_0$ are determined from a molecular orbital calculation using a finite electric field perturbation technique. Briefly, in an electric field $\mathbf{F}$ with a perturbed Hamiltonian $\mathcal{H} = \mathcal{H}^0 - \mu\cdot\mathbf{F}$ and electronic energy $\epsilon = \langle\psi|\mathcal{H}|\psi\rangle$, the electronic contribution to the dipole

(21) Barron, L. D. *J. Chem. Soc., Perkin Trans. 2* **1977**, 1074.
(22) Barron, L. D.; Torrance, J. F.; Vrbancich, J. *J. Raman Spectrosc.* **1982**, *13*, 171.
(23) Dobish, P. A. *QCPE* **1969**, *11*, 141.

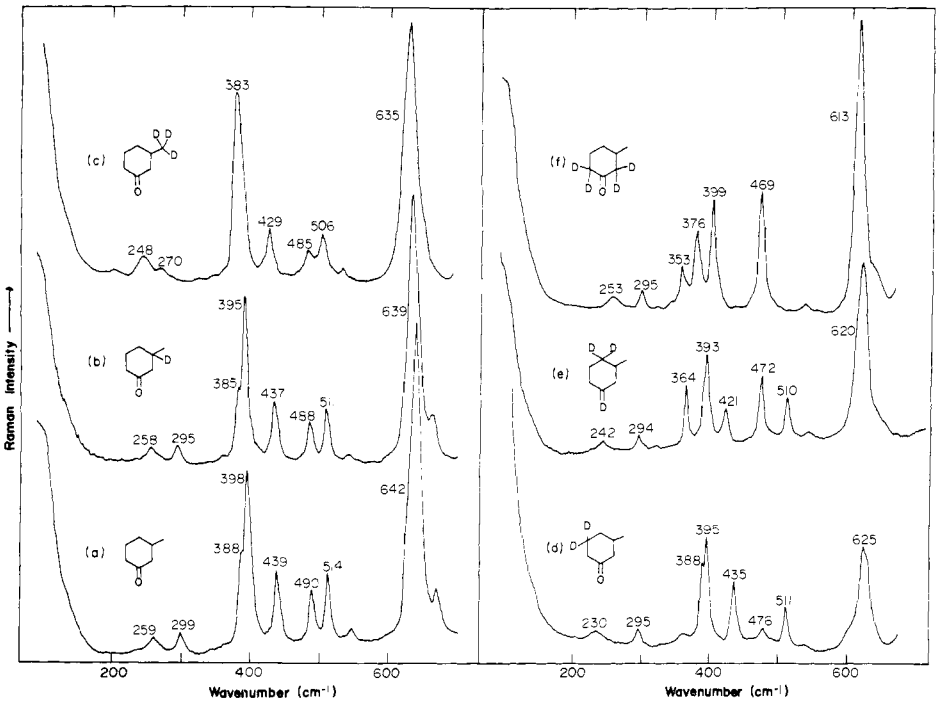

Figure 1. Raman spectra of the skeletal vibrations of (a) 3-methylcyclohexanone, (b) 3-methylcyclohexanone-*3*-d_1, (c) 3-(methyl-d_3)-cyclohexanone, (d) 3-methylcyclohexanone-*5,5*-d_2, (e) 3-methylcyclohexanone-*4,4*-d_2, and (f) 3-methylcyclohexanone-*2,2,6,6*-d_4 as neat liquids. The intensities have not been scaled.

moment derivative is derived as a finite electric field derivative of the electronic potential energy gradient

$$\left(\frac{\partial \mu_\sigma^{el}}{\partial R_{n\rho}}\right)_0 = -\left[\frac{\partial}{\partial R_{n\rho}}\left(\frac{\partial \epsilon}{\partial F_\sigma}\right)\right]_0 \approx -\left[\frac{\Delta}{\Delta F_\sigma}\left(\frac{\partial \epsilon}{\partial R_{n\rho}}\right)\right]_0 \quad (8)$$

and the polarizability derivative is calculated as a second finite derivative,

$$\left(\frac{\partial \alpha_{\alpha\beta}}{\partial R_{n\rho}}\right)_0 = \left[\frac{\partial}{\partial R_{n\rho}}\left(\frac{\partial \mu_\alpha^{el}}{\partial F_\beta}\right)\right]_0 = \left[\frac{\partial}{\partial F_\beta}\left(\frac{\partial \mu_\alpha^{el}}{\partial R_{n\rho}}\right)\right]_0 \approx -\left[\frac{\Delta}{\Delta F_\beta}\left(\frac{\Delta}{\Delta F_\alpha}\frac{\partial \epsilon}{\partial R_{n\rho}}\right)\right]_0 \quad (9)$$

The calculations presented below were carried out using CNDO wave functions as described previously for VCD, requiring an equilibrium and 18 electric field perturbed SCF–MO calculations, all at the equilibrium geometry.[16] The Raman atomic polar tensor elements generated from the MO calculation were stored for use in the Raman and ROA intensity calculations as the force field was refined.

Results

The Raman spectra of 3-methylcyclohexanone and the five deuterated isotopomers in the 100–700-cm^{-1} region are shown in Figure 1. The Raman optical activity spectrum of (+)-(3*R*)-methylcyclohexanone, adapted from Barron,[2,3,21,22] is compared with the corresponding Raman spectrum in Figure 2. Two low-frequency transitions at ~112 and ~140 cm^{-1} are obscured by the Rayleigh wing in Figures 1 and 2. Any shifts in these two frequencies due to isotopic substitution appeared to be small, but could not be accurately determined. The frequencies of bands corresponding to skeletal fundamentals for each isotope are indicated in Figure 1 and listed in Table I. Unlabeled weak features are attributed to overtone or combination bands.

Several features of the ROA spectrum are of particular interest: the two large, fairly sharp bisignate ROA couplets corresponding to transitions at 514 and 490 cm^{-1} and at 398 and 388 cm^{-1}, and the broad positive feature encompassing the 299- and 259-cm^{-1} transitions and negative feature at 140 cm^{-1} which may also

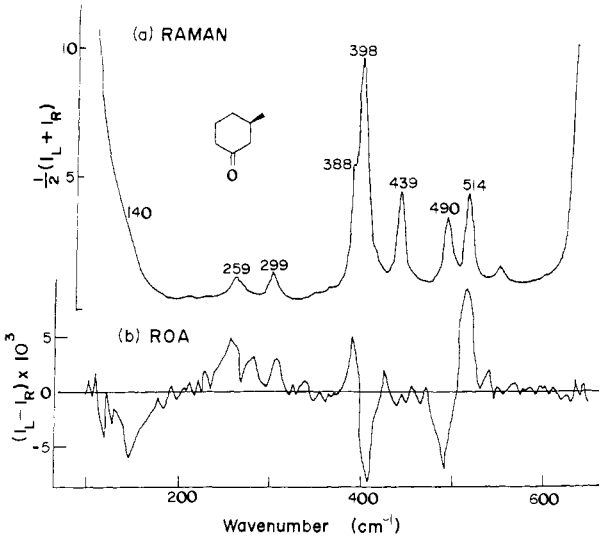

Figure 2. Comparison of the Raman and Raman optical activity spectra of the skeletal vibrations of (+)-(3*R*)-methylcyclohexanone. The ROA spectrum (b) has been redrawn with a linear ordinate (I_L - I_R) from the data in ref 2.

constitute a couplet. Some significant ROA is also observed in regions where only very weak Raman scattering occurs.

There are 11 skeletal fundamentals for 3-methylcyclohexanone occurring below 700 cm^{-1}. Although 3-methylcyclohexanone possesses no symmetry elements and thus there are no symmetry restrictions on the makeup of the normal modes, it is quite useful for our subsequent analysis to consider a set of simpler achiral motions which combine to generate the fundamental vibrations in 3-methylcyclohexanone. These motions are depicted schematically in Figure 3. In the diagrams, the relative sense and magnitude of an angle deformation in a given mode is indicated by the integer adjacent to the central atom in the angle, a positive value denoting an increase in angle. For the other modes, the arrows represent the direction and relative magnitude of nuclear displacement. The C_6 ring alone, in the chair conformation, has D_{3d} symmetry, and the six CCC angle bending coordinates and

Table I. Observed and Calculated Skeletal Frequencies (cm^{-1}) of 3-Methylcyclohexanone and Deuterated Isotopomers

3-methylcyclohexanone		3-methylcyclohexanone-*4,4-d_2*		3-methylcyclohexanone-*5,5-d_2*	
obsd	calcd	obsd	calcd	obsd	calcd
642	639	620	617	625	632
514	517	510	514	511	509
490	484	472	468	476	467
439	444	421	437	435	433
398	397	393	391	395	393
388	388	364	352	388	382
299	301	294	293	295	288
259	257	242	247	230	236
	219		219		216
140	139		137		138
112	114		111		113
3-methylcyclohexanone-*2,2,6,6-d_4*		3-(methyl-d_3)-cyclohexanone		3-methylcyclohexanone-*3-d_1*	
obsd	calcd	obsd	calcd	obsd	calcd
613	612	635	633	639	638
469	485	506	508	511	514
	463	485	478	488	482
399	385	429	441	437	443
376	375	383	392	395	394
353	369		375	385	385
295	292	270	285	295	298
253	249	248	242	258	256
	218		160		219
	130		132		138
	107		111		113

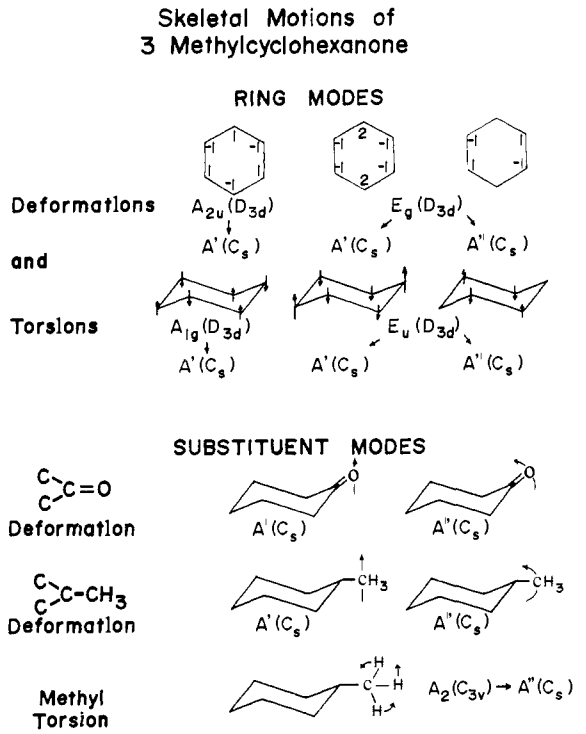

Figure 3. Descriptive representation of the ring and substituent motions involved in the skeletal modes of 3-methylcyclohexanone.

six CC–CC torsion coordinates of the ring generate 12 symmetry coordinates, six of which are redundant. The six remaining coordinates, of species A_{1g}, A_{2u}, E_g, and E_u, each a linear combination of torsion and deformation, correlate with 4A′ and 2A″ species when the symmetry is reduced to C_s, as, for example in cyclohexanone. In Figure 3 we have illustrated the form of either the torsion or deformation of each species. The substituents contribute five additional skeletal motions. The carbonyl and methyl group can each undergo a deformation in a direction parallel to the ring C_3 axis, an A′-type motion under C_s symmetry, or perpendicular to the ring C_3 axis, a motion of species A″. Finally the methyl group itself can undergo a torsional motion (A″) relative to the ring.

Table II. Skeletal Force Constants[a] for 3-Methylcyclohexanone

internal coordinate	initial force field[a-c]	refined force field
C-C(1)-C	1.11	1.11
C-C(2)-C	1.068	0.550
C-C(6)-C	1.068	0.550
C-C(3)-C	1.024	1.20
C-C(4)-C	1.024	1.30
C-C(5)-C	1.024	0.88
C-C-O	0.919	0.936
C-CO-C out of plane	0.534	0.625
C-C-C (Me)	1.084	0.780
CC-CC(=O) torsion	0.008	0.010
CC-CC torsion	0.093	0.170
methyl torsion	0.024	0.010

[a] Force constant units are mdyn Å (10^{-18} N m). [b] Cyclohexanone force constants, ref 19. [c] Methyl group force constants, ref 24.

Normal Coordinate Analysis

Both the qualitative understanding of the types of vibrational motions and the mechanisms which generate specific ROA features, and the application of the more quantitative intensity models require an accurate description of the normal modes of the molecule. A complete normal coordinate analysis with sufficient accuracy of a large low-symmetry molecule such as 3-methylcyclohexanone has proved to be a formidable task, even with the availability of both Raman and infrared spectra of specifically deuterated species. The major difficulties lie in distinguishing possibly weak fundamentals from numerous overtone and combination bands which may be Fermi resonance enhanced, and in the fact that with the exception of CH stretches, methyl deformations and methylene scissors motions, the internal coordinates, are heavily mixed.[19]

Since the 11 vibrations below 650 cm^{-1} are dominated by CCC, CCO, and C–CO–C deformations and ring or methyl torsions, with only minor contributions from methylene rocking and methine deformation, we have been successful in calculating the skeletal modes by carefully refining a restricted set of force constants. Our approach has been to (1) transfer valence force constants from previous force-field calculations of cyclohexanone[19] and the methyl group;[24] (2) retain the transferred off-diagonal interaction force constants; (3) adjust the HCH and HCC angle bending force constants and C—C and C=O stretching force constants if desired to give more reasonable calculated frequencies between 700 and 1750 cm^{-1}; and finally (4) carefully adjust the diagonal CCC, C–CO–C, and CCO angle bending constants and the ring and methyl torsion force constants until good agreement with experiment both in calculated frequencies and calculated q_p values was obtained for the 11 low-frequency modes. The various reasonable force constant sets chosen in step 3 affected to varying degrees the frequencies and intensities calculated for the skeletal modes, but not the descriptive picture of individual modes.

Most critical to our analysis were the refinements in step 4. Standard perturbation procedures such as FPERT did not tend toward reasonable convergence or force constants. Instead a normal coordinate analysis was carried out in Cartesian coordinates wherein the relative Cartesian nuclear trajectories $(\partial \boldsymbol{R}_n/\partial Q_a)_0$ are output directly. The molecule was assumed to be in the most stable chair conformation with a staggered equatorial methyl group. The force constants of step 4 were adjusted individually, simultaneously monitoring the effect on frequency and ROA intensity agreement. Several major changes from the transferred force fields are required (Table II). First the CCC

(24) Snyder, R. G.; Schachtschneider, J. H. *Spectrochim. Acta* **1965**, *21*, 195.

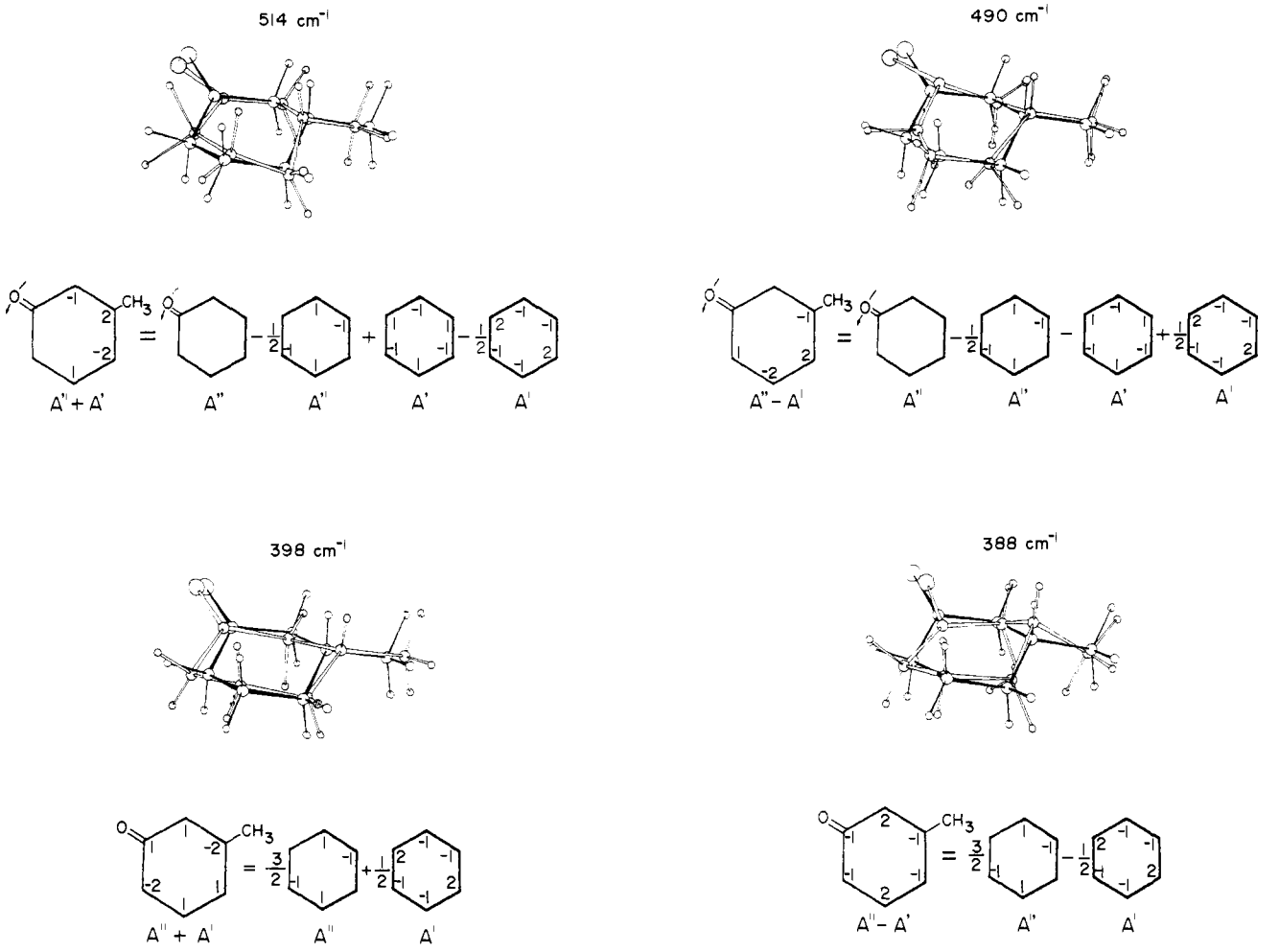

Figure 4. Stereoprojections of 3-methylcyclohexanone showing the equilibrium geometry (white circles and black bonds) and vibrationally displaced structure (shaded circles and white bonds) for the normal modes at 514, 490, 398, and 388 cm^{-1}. Shown schematically beneath each mode is the predominant pattern of motion and the linear combination of achiral motions which generate the vibration.

angle bending force constant for the C(2) and C(6) carbons was considerably decreased and the CC–CC torsion force constants about the four ring C–C bonds not adjacent to the carbonyl group were increased. The CCC(Me) angle bending force constant was adjusted such that the largest contribution from CCC(Me) deformation occurred at 299 cm^{-1}, the band most affected by deuteration at the methyl group. The remaining angle deformation constants were then varied slightly to give calculated bands close to the ten most prominent low-frequency features of 3-methylcyclohexanone.

No Raman band is observed which shows the factor of ~ 1.4 decrease in frequency upon methyl deuteration expected for the methyl torsion. Methyl torsion modes, deriving from motion of locally Raman inactive A_2 species, are normally weak or unobserved in Raman spectra. Several lines of evidence point to assignment of this mode near 220 cm^{-1} in 3-methylcyclohexanone. The methyl torsion mode in unstrained systems commonly occurs in this region.[25] For example, in propanal, in the gas phase, the methyl torsion is assigned between 210 and 220 cm^{-1} depending on conformation.[26] In a liquid, this frequency may be higher. In 3-methylcyclohexanone no Raman band is observed near 220 cm^{-1}; however, Barron observed significant positive ROA intensity at 224 cm^{-1}, part of the broad ROA feature centered at 258 cm^{-1}, and a sharp positive ROA feature at 423 cm^{-1}, corresponding to a weak shoulder in the Raman spectrum. Methyl torsion overtones, with local A_1 symmetry, are frequently observed in gas-phase Raman spectra, with greater intensity than the fundamental.[25] The ROA feature at 423 cm^{-1} lies in the region in which a first overtone of a methyl torsion near 220 cm^{-1} should occur. In the Raman spectrum of 3-methylcyclohexanone-*2,2,6,6-d*$_4$ no interfering fundamentals lie near 440 cm^{-1}, and a very weak Raman band at 435 cm^{-1} is observed in that isotopomer. In the methyl deuterated isotopomer a weak band which can be attributed to the corresponding deuterated methyl torsion overtone is observed at 328 cm^{-1}. We have therefore adjusted the methyl torsion force constant to generate a mode in the 220-cm^{-1} region.

In Table I we compare the observed and calculated frequencies for the six isotopic species included in this study. The average deviation $|\nu_{calcd} - \nu_{obsd}|$ for 50 observed bands is 5 cm^{-1}. The force field (Table II) used to generate the frequencies in Table I is the one which simultaneously gave the best calculated q_p values for the ROA spectrum. We were also able to obtain similar agreement in frequency with several other sets of force constants, which, while not altering the general form of each vibration, did not reproduce the observed ROA pattern as well.

Descriptive Interpretation of the ROA Spectrum

Since numerous force constants and internal coordinates contribute to each skeletal mode, the potential energy distribution in terms of percent contribution of diagonal force constants provides an incomplete description of these vibrations. Of prime utility to our qualitative understanding of the sources of ROA intensity are the comparisons of stereoprojections of the molecule at equilibrium and distorted along each normal mode in Figures 4 to 6. We have also calculated the relative numerical changes in valence and dihedral angles for each mode. Analysis of this information has led to the schematic approximate description of

(25) Groner, P.; Sullivan, J. F.; Durig, J. R. In "Vibrational Spectra and Structure"; Durig, J. R., Ed.; Elsevier: Amsterdam, 1981; Vol. 9, p 405.
(26) Durig, J. R.; Compton, D. A. C.; McArver, A. Q. *J. Chem. Phys.* **1980**, *73*, 719.

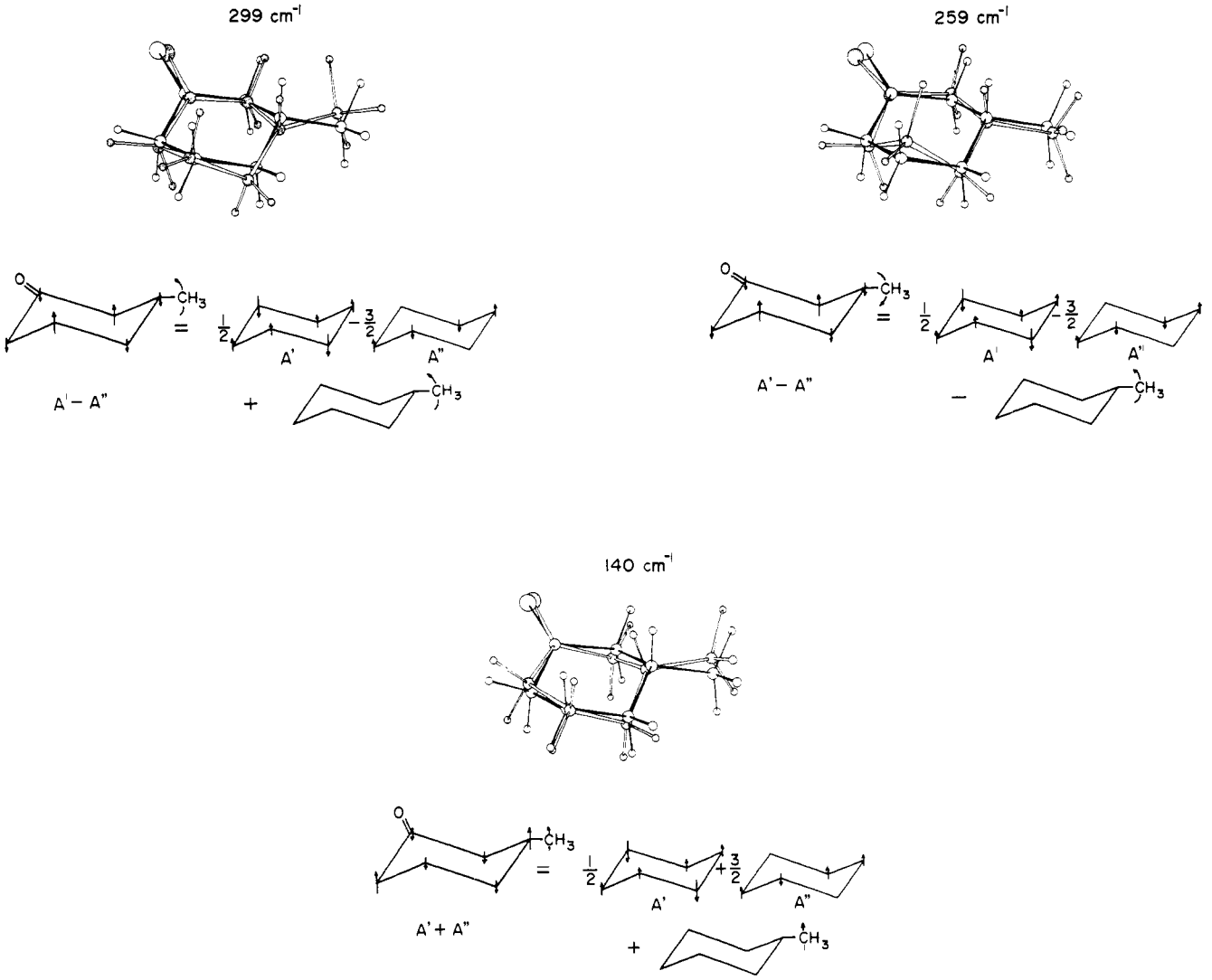

Figure 5. Stereoprojections and description of the skeletal motions of 3-methylcyclohexanone at 299, 259, and 140 cm^{-1} (see Figure 4).

the predominate motions involved in each mode, given at the left beneath each stereoprojection. These, in turn, can be generated by the linear combinations (shown to the right) of the simple achiral motions in Figure 3. In Figures 4 to 6, the species notations are for a C_s structure with the symmetry plane bisecting the ring through the C=O group. For simplicity, smaller contributions from methylene rocking motion, ring deformation, and/or torsion have not been included. These enter with the same symmetry combinations as the major motion shown.

This method of describing the skeletal vibrations of 3-methylcyclohexanone leads directly to an interpretation of the ROA spectrum in terms of chiral perturbation of inherently achiral vibrations discussed above. The largest perturbation of the ring is due to the carbonyl group, and we take the achiral structure to be cyclohexanone (C_s) perturbed by the chiral vibrational potential of the methyl group in the 3 position.

The ROA couplet at 514 and 490 cm^{-1} arises from A" (in-plane) carbonyl deformation coupled in and out of phase with ring deformation. The overall motion (Figure 4) can be approximated as a coupled (A" + A') and (A" − A') vibrational pair, which gives rise to an ROA couplet through terms as in eq 6. In the same way, the ring motions involved in the modes at 398 and 388 cm^{-1} can be described as an (A" + A') and (A" − A') pair, which in this case are ring deformations of similar form which are symmetric to vertical planes rotated −60 and +60°, respectively, relative to the symmetry plane of cyclohexanone. The A' deformation of the CCC(Me) angle also contributes to the mode at 388 cm^{-1}. Again, these motions would be predicted to generate an ROA couplet, as observed.

The broad positive and negative ROA features below 300 cm^{-1} are also qualitatively explained by this model. These modes primarily involve ring torsions. The two bands at 299 and 259 cm^{-1} are seen to arise from the A" deformation of the CCC(Me) angle coupled in and out of phase with the same type of ring torsional motion, whereas the band at 140 cm^{-1} is due to A' CCC(Me) deformation coupled to ring torsion. The ring torsions occurring in the 299- and 259-cm^{-1} modes and in the 140-cm^{-1} mode again can be described as an (A' ± A") pair of the same type that gives rise to the ring deformation couplet at 398 and 388 cm^{-1}. In this view it is the chiral mixing of the A' and A" ring torsional modes which gives rise to the low wavenumber couplet, rather than mixing of the perpendicular CCC(Me) deformations as had been suggested by Barron, although the latter effect may also be contributing.[2]

The approximate motions involved in the remaining four skeletal modes are depicted in Figure 6. The vibrations at 642 and 112 cm^{-1}, although widely separated in frequency, both contain contributions from A' (out of plane) C–CO–C deformation. The ring motions in these two vibrations appear to have opposite phase (for the same sense of carbonyl deformation) and to retain primarily A' character relative to a cyclohexanone framework. Although this description predicts weak ROA intensity in both these modes, comparison with experiment is difficult, since the 642-cm^{-1} Raman band is intense and highly polarized, rendering the ROA prone to artifact, and the 112-cm^{-1} band lies within the Rayleigh wing.

The mode at 439 cm^{-1} arises from quite complex motion (Figure 6) and can best be approximated by a combination of four types of ring deformation, one type of ring torsion and some in-plane

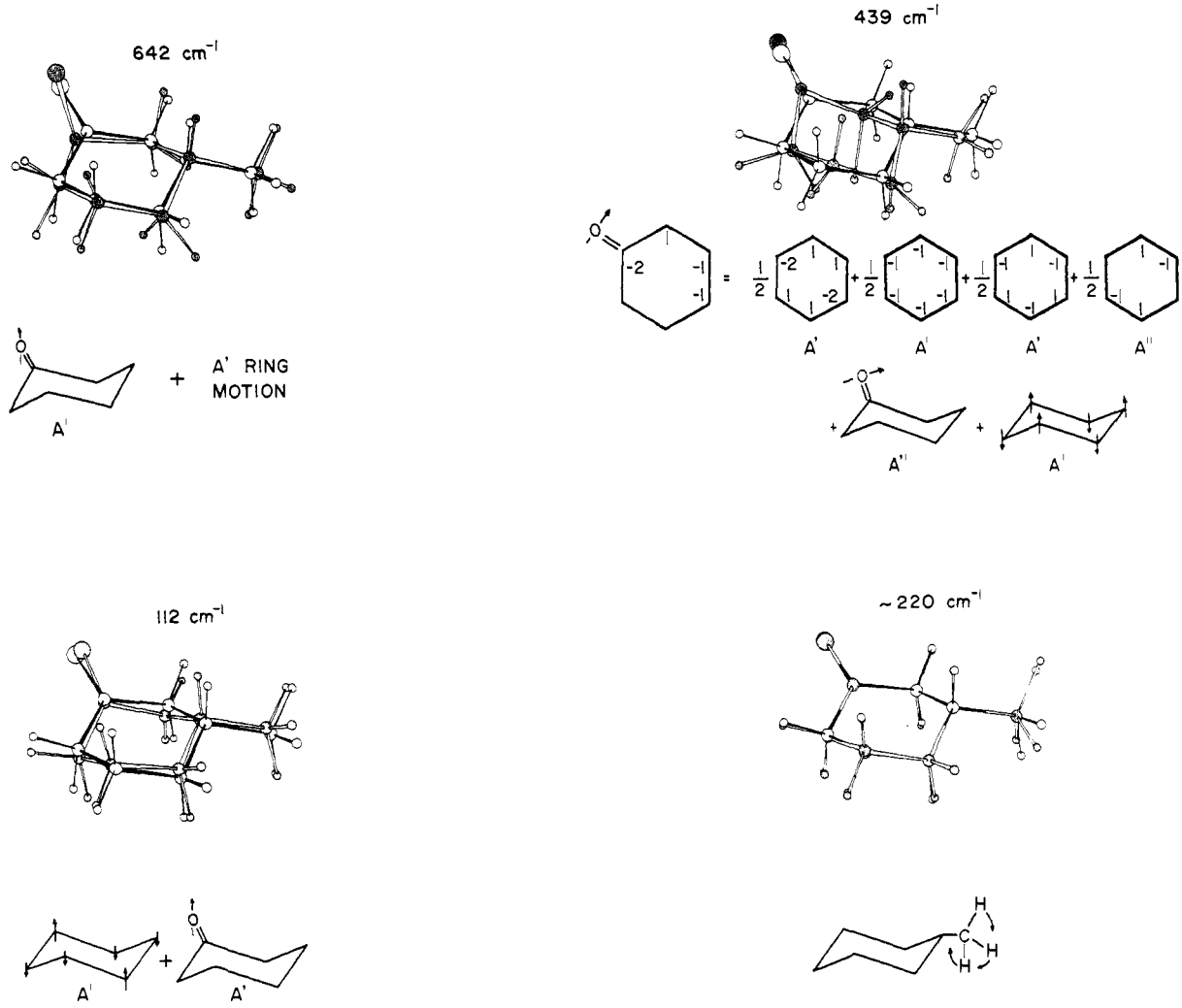

Figure 6. Stereoprojections and description of the skeletal vibrations of 3-methylcyclohexanone at 642, 439, 112, and ~220 cm^{-1} (see Figure 4).

Table III. Comparison of Observed and Calculated Frequencies and Assignments of the Skeletal Motions of Cyclohexanone, Methylcyclohexane, and 3-Methylcyclohexanone

cyclohexanone[a]			3-methylcyclohexanone[b]			methylcyclohexane[c]		
obsd (cm^{-1})	sym[d]	calcd (cm^{-1})	obsd (cm^{-1})	sym[d]	calcd (cm^{-1})	obsd (cm^{-1})	sym[d]	calcd (cm^{-1})
652	A'	643	642	~A'	639			
	A'	488	514	(A' ± A'')	517	546	A'	537
490	A''	484	490		484			
460	A''	452	440	A', A''	444	444	A''	458
411	A'	421	398	(A' ± A'')	397		A'	427
			388		388	406	A'	418
			299	(A' − A'')	301	339	A''	332
313	A'	295	259		257	313	A'	321
			220	A''	219		A''	194
189	A''	200	140	(A' + A'')	139	237[e]	A''	233
105	A'	127	112	~A'	114	165[e]	A'	151

[a] Reference 19. [b] This work. [c] Reference 24. [d] Assigned species for C_s symmetry. Species notation for 3-methylcyclohexanone refers to the symmetry plane of cyclohexanone. [e] Reference 29.

CCO deformation. It does not constitute a member of a perturbed pair, and no significant ROA intensity is observed at this frequency.

The remaining skeletal mode is the methyl torsion. As noted above, this mode is weak and its position uncertain. Barron has speculated that methyl torsions might exhibit significant ROA via an inertial mechanism[2,27] and has identified an ROA feature due to in phase methyl torsion in (2*S*,3*S*)-(−)-2,3-epoxybutane at 182 cm^{-1}.[28] We have tentatively assigned the methyl torsion in 3-methylcyclohexanone at 220 cm^{-1}; unless the mode is placed quite near in frequency to another fundamental, the calculations yield a mode which is not mixed with other coordinates. As noted by Barron, any optical activity in this mode is due to motion of the chiral cyclohexanone frame which compensates for methyl torsion to yield zero net angular momentum. We have noted the possible assignment of positive ROA contribution from the methyl torsion and methyl torsion overtone in 3-methylcyclohexanone.

(27) Barron, L. D.; Buckingham, A. D. *J. Am. Chem. Soc.* **1979**, *101*, 1979.

(28) Barron, L. D.; Vrbancich, *J. Mol. Phys.* **1983**, *48*, 833.

A comparison of the skeletal frequencies and assignments for 3-methylcyclohexanone, cyclohexanone, and methylcyclohexane shown in Table III also lends support to our assignments and suggested mechanism for ROA intensity. The data for the two achiral species were taken from the literature.[19,24] In cyclohexanone the modes at 652 and 490 cm^{-1} are attributed largely to out-of-plane (A″) and in-plane (A′) carbonyl deformation, respectively. In methylcyclohexane, the "in-plane" CCC(Me) deformation (A″) is assigned at 339 cm^{-1}, while the A′ CCC(Me) deformation contributes to some extent to all the A′ modes below 410 cm^{-1}. The methyl torsion frequency, although not observed, is calculated at 194 cm^{-1}. From the stereoprojections of the 3-methylcyclohexanone vibrations, Figures 4–6, the corresponding substituent motions are seen to contribute in the same regions. When the symmetry is lowered by the presence of both the methyl and carbonyl groups, the ring motions in the same region which are initially symmetric and antisymmetric to the symmetry plane can mix, giving rise to the 3-methylcyclohexanone modes. The species notation given for 3-methylcyclohexanone corresponds to the symmetry plane in cyclohexanone, since our analysis shows that the methyl group induces the weaker perturbation on the symmetry of the ring motions in the disubstituted ring.

In contrast to the suggestion of Barron attributing the ROA couplets to chiral perturbation by the ring mixing the in- and out-of-plane substituent deformations, our analysis points to chiral perturbation by the methyl group mixing A′ and A″ ring motions in cyclohexanone as the primary source of Raman optical activity in 3-methylcyclohexanone.

Interpretation of ROA Spectra in Similar Molecules

A number of molecules for which ROA spectra have been previously reported are structurally similar to 3-methylcyclohexanone, and our study finds direct application to the interpretation of these spectra.

One group of molecules contains a carbonyl group connected to a six-membered ring substituted at the 3 position ((+)-pulegone,[10] (+)-camphor,[21] (+)-3-bromocamphor,[21] and (+)-nopinone[22]). The ROA spectra of each of these molecules includes a conservative couplet of the same sense centered at about 500 cm^{-1}. This couplet is not observed when the carbonyl is replaced by a hydroxyl or vinylidene group, and is less distinct or absent in molecules with a larger number of substituents or with a double bond in the ring between C(5) and C(6) ((−)-β-inene,[22] (−)-3-methylmethylenecyclohexane,[22] (−)-5-methylcyclohex-2-en-1-one,[22] (−)-3-bromocamphor-9-sulfonic acid,[21] etc.). Our descritpion of these two modes as A″ carbonyl deformation coupled with an (A″ + A′), (A′ − A″) pair of ring deformation is consistent with these experimental observations, since both types of ring substitutions above would alter the modes by elminating the contributions from the carbonyl or changing the ring deformations involved, respectively. The ROA couplet at 400 cm^{-1} is, as might be expected from the ring deformations assigned in 3-methylcyclohexanone, quite sensitive to any alteration in the ring, and is possibly present in the ROA spectrum of (*R*)-(−)-3-methylmethylenecyclohexane,[22] but not in the ROA spectra of any of the other molecules. Finally, the broad low-frequency ROA features in 3-methylcyclohexanone, which mainly involves CCC(Me) deformation coupled to ring torsion, are observed for molecules with 3-methyl-substituted rings, but not with other or additional ring substituents.

Intensity Calculations

We have used the Raman atomic polar tensor model to calculate both Raman and ROA intensities for the skeletal modes of (+)-(3*R*)-methylcyclohexanone. The polarizability tensor dervatives derived from CNDO wave functions using the finite electric field perturbation method (eq 8 and 9) did not yield calculated relative depolarized Raman intensities which agreed well with the experimental spectrum, especially below 400 cm^{-1}. Since both the calculated Raman intensities and circular intensity differences (I_L - I_R) were too low in this region, we have chosen to compare the experimental and calculated intensity ratio, q_p (eq 1 and 2). The results of our best calculation are presented in Table IV. For this force field agreement in sign and generally satisfactory agreement in magnitude is obtained for all the modes. In particular, all the couplets are reproduced with the correct sign relationship.

Table IV. Comparison of Experimental Chirality Numbers for the Skeletal Vibrations of (+)-(3*R*)-Methylcyclohexanone and Calculated Values Using the Raman Atomic Polar Tensor Model of ROA

observed[a]		calculated	
freq (cm^{-1})	$q_p \times 10^3$	freq (cm^{-1})	$q_p \times 10^3$
514	2.2	517	0.26
490	−1.9	484	−1.4
439	−0.28	444	−0.25
398	−1.2	399	−0.94
388	0.94	388	1.9
299	1.2	301	1.3
259	4.6	257	4.4
(220)	(+)	219	0.87
140	−4	139	−4.1
112	−1	114	−3.2

[a] Reference 19.

As described above, the set of Raman atomic polar tensor elements obtained from a molecular orbital calculation at the equilibrium geometry can be used to calculate ROA and Raman intesity for all the normal modes in a single calculation, and therefore the effect on intensities of changes in the force field is readily monitored. We observed that even though the overall descriptive nature of the modes did not change significantly when force constants were varied slightly, the calculated q_p values (including sign) were extremely sensitive to the precise nature of the nuclear trajectories. For example, the calculated sense of the couplet at 398 and 388 cm^{-1} could be reversed by decreasing the force constant for C–C(3)–C deformation and increasing that for C–C(5)–C deformation, even though the calculated frequencies and approximate mode description did not change. Since the internal coordinates are heavily mixed in the skeletal vibrations, changing a single force constant affects the intensity calculation for several modes. Force fields which altered the descriptive nature of any of the modes in terms of the coupling of achiral vibrations also resulted in poor agreement in calculated ROA intensities throughout the region.

The restrictions which the ROA calculations apparently place on the force field have also been encountered in our VCD calculations in the CH stretching region, where, in a molecule such as 3-methylcyclohexanone numerous CH stretching modes occur within a ~100-cm^{-1} region, and the VCD is generated by weak coupling among the CH stretches on adjacent carbon atoms. Some of the sensitivity in the ROA calculation may derive from the approximate nature of the ROA–APT model itself, and from the difficulties in using CNDO wave functions to calculate Raman intensities. However, the discussion of the previous section provides experimental evidence for the influence on the skeletal motions and their ROA spectra of structural perturbations which alter the force field. Moreover, the agreement in Table IV for the entire low-frequency region, using a force field which also allows a complete descriptive interpretation based on chirally perturbed motions, supports the validity and usefulness of the ROA–APT model. As has been our experience with the VCD–APT model, even if more precise models become available, we expect the ROA–APT method to find application as an efficient and inexpensive method for interpreting ROA spectra and for using ROA intensities to help refine the vibrational force fields for chiral molecules.

Conclusions

Our analysis of the Raman optical activity in (+)-(3*R*)-methylcyclohexanone has shown that the coupling of vibrations due to chiral perturbation is a major source for the generation of ROA couplets and should be considered in interpreting the

(29) Zhizhin, G. N.; Sterin, Kh. E. In ref 25, p 195.

ROA in other spectral regions of this molecule and in other molecules. In particular, we have presented evidence for the importance of vibrational mixing of ring motions of similar frequency but different symmetry species induced by chiral substitution and coupling with motions of the substituent. It seems probable that, as is observed in VCD, intense ROA arises from nuclear motion spread out over the chiral frame, rather than from localized vibrations. For example, the prominent ROA couplet observed at 968 and 942 cm^{-1} in 3-methylcyclohexanone[2] (corresponding to Raman bands at 969, 960, and 946 cm^{-1}) lies in the frequency region for the A′ methyl rock in methylcyclohexane[24] (971 cm^{-1}) and for the cyclohexanone[19] modes at 990 (A′) and 907 cm^{-1} (A″) which involve C–C stretch and CCH deformation in the ring. The ROA couplet probably arises from chiral vibrational mixing of these modes, rather than from mixing of the A′ and A″ methyl rocks as has been previously proposed.[3,18] The couplet near 1450 cm^{-1} in 1-substituted arylethanes,[4,5,30-32] another important example, lies in the region where both the two components of the antisymmetric methyl deformation and two substituted benzene modes, 19a (a_1) and 19b (b_2) in Wilson's notation,[33] occur. The couplet is absent both in trideuterio-[8] or trifluoro-substituted[32] species and in (*p*-bromophenyl)ethylamine.[32] As previously suggested,[32] a dynamic interaction of the methyl and phenyl modes is require to explain the ROA couplet, rather than static splitting of the methyl degeneracy.[4] Hug[5] postulated either an equal admixture of the 19b mode with the two methyl deformations or a biphasic coupling of 19b with one of the methyl deformation components. Since all four modes in this region can interact, a couplet generated by methyl deformation mixed with in-phase contributions of 19b and 19a and a second methyl deformation coupled to out-of-phase 19a, 19b contributions is also a possible explanation, in line with our 3-methylcyclohexanone results. Similarly, the substituted benzene modes 17a (a_2) and 17b (b_1) interacting with the methyl rock or the modes 16a (a_2) and 16b (b_1) interacting with chiral substituent motion are types of chirally induced mixing which may give rise to the ROA features near 1000 cm^{-1} and 450 cm^{-1} in chirally substituted arylethanes.

This study also points to the usefulness of stereoprojections of vibrational displacements in identifying patterns of motion and coupling in the normal modes of large, low-symmetry molecules. We note, in particular, that symmetry reduction need not drastically alter the form of vibrational motion.

Finally, we have presented the first theoretical calculation of ROA intensity which agrees well with experiment over a fairly large spectral region. The ADI and bond polarizability models may also yield good results given an accurate force field, but we emphasize here that, unlike these two models, the ROA–APT model requires no empirical parameters once a molecular orbital scheme has been chosen. Furthermore, the ROA–APT model does not require division of the molecule into local polarizability units. Hopefully, correlation between 3-methylcyclohexanone, methylcyclohexane, and cyclohexanone spectra will also aid in the interpretation of the more complex mid-infrared and Raman regions (1750–700 cm^{-1}) in which both ROA and FTIR–VCD[34] data for 3-methylcyclohexanone have been recorded, and in which the APT models of both ROA and VCD can be simultaneously employed and evaluated.

Acknowledgment is given for financial support of this research by grants from the National Institutes of Health, GM-23567, and the National Science Foundation, CHE-83-02416.

(30) Barron, L. D. *Nature (London)* **1975**, *255*, 458.
(31) Barron, L. D.; Clark, B. P. *J. Chem. Res. Suppl.* **1979**, *36*.
(32) Barron, L. D. *J. Chem. Soc., Perkin Trans. 2* **1977**, 1790.
(33) Dollish, F. R.; Fateley, W. G.; Bentley, F. F. "Characteristic Raman Frequencies of Organic Compounds"; Wiley: New York, 1974; Chapter 13.
(34) Lipp, E. D.; Zimba, C. G.; Nafie, L. A. *Chem. Phys. Lett.* **1982**, *90*, 1.

Gas-Phase Reactions of FeO^+ with Hydrocarbons

T. C. Jackson, D. B. Jacobson, and B. S. Freiser*

Contribution from the Department of Chemistry, Purdue University, West Lafayette, Indiana 47907. *Received August 15, 1983*

Abstract: The reactions of FeO^+ with linear alkanes, cyclic alkanes, and branched alkanes are presented. In general from the reactions observed, it appears that FeO^+ is more reactive toward alkanes than Fe^+ which is due mainly to the greater reaction exothermicity involved in H_2O loss. The majority of the products observed may be explained by initial C–H insertion and loss of H_2O to produce an activated Fe^+–olefin complex which subsequently decomposes. An alternative mechanism involving C–C insertion, however, cannot be ruled out and is in fact supported by observation of radical loss products. These radical loss products dominate for systems in which C–H insertion pathways are inhibited by the absence of β hydrogens.

While transition-metal ion chemistry has been extensively studied in solution, only recently has much attention been given to the gas-phase chemistry of these species. These recent studies on the reactions of gas-phase transition-metal ions with various organic compounds have shown this chemistry to be both rich and unusual, exhibiting oxidative addition across carbon–halogen,[1-3] carbon–oxygen,[2,4,5] carbon–hydrogen,[2,6-9] and carbon–carbon[2,6-9] bonds. In addition, these studies have resulted in kinetic, mechanistic, and thermodynamic data about the metal ions themselves, and also about the reactions in which they take part. A major focus of these studies has been the determination of reaction mechanisms, and this has been greatly facilitated by the

(1) Allison, J.; Ridge, D. P. *J. Am. Chem. Soc.* **1976**, *98*, 7445.
(2) Allison, J.; Ridge, D. P. *J. Am. Chem. Soc.* **1979**, *101*, 4998.
(3) Uppal, J. S.; Staley, R. H. *J. Am. Chem. Soc.* **1980**, *102*, 4144.
(4) Allison, J.; Ridge, D. P. *J. Am. Chem. Soc.* **1978**, *100*, 163.
(5) Burnier, R. C.; Byrd, G. D.; Freiser, B. S. *J. Am. Chem. Soc.* **1981**, *103*, 4360.
(6) (a) Allison, J.; Freas, R. B.; Ridge, D. P. *J. Am. Chem. Soc.* **1979**, *101*, 1332. (b) Freas, R. B.; Ridge, D. P. *Ibid.* **1980**, *102*, 7129.
(7) (a) Armentrout, P. B.; Beauchamp, J. L. *J. Am. Chem. Soc.* **1981**, *103*, 784. (b) Halle, L. F.; Armentrout, P. B.; Beauchamp, J. L. *Organometallics* **1982**, *1*, 963.
(8) (a) Byrd, G. D.; Burnier, R. C.; Freiser, B. S. *J. Am. Chem. Soc.* **1982**, *104*, 3565. (b) Byrd, G. D.; Freiser, B. S. *Ibid.* **1982**, *104*, 5944.
(9) (a) Jacobson, D. B.; Freiser, B. S. *J. Am. Chem. Soc.* **1983**, *105*, 736. (b) Jacobson, D. B.; Freiser, B. S. *Ibid.* **1983**, *105*, 5197.

0002-7863/84/1506-1252$01.50/0